Journal of Inflammation Research

Dovepress
Taylor & Francis Group

Open Access Full Text Article

ORIGINAL RESEARCH

NCF2 as a Novel Diagnostic Biomarker in Ulcerative Colitis: Linking Macrophage Infiltration to Immune Dysregulation via Multi-Omics Analysis

Fang Zhang[1,2,*], Jianwei Zhu[3,*], Haiyan Liu[4,*], Jianlan Ye[1], Yuanyuan Li[5], Bingcheng Wang[1]

[1]Department of Outpatient, Jinling Hospital, Affiliated Hospital of Medical School, Nanjing University, Nanjing, People's Republic of China; [2]Department of Gastroenterology, The Affiliated Hospital of Yangzhou University, Yangzhou University, Yangzhou, People's Republic of China; [3]Department of Gastroenterology Shanghai Tenth People's Hospital, Tongji University School of Medicine, Shanghai, People's Republic of China; [4]Department of Rehabilitation medicine, Eastern Theater Command Air Force Hospital, Nanjing, People's Republic of China; [5]Department of Pharmacy, Eastern Theater Command Air Force Hospital, Nanjing, People's Republic of China

*These authors contributed equally to this work

Correspondence: Bingcheng Wang; Yuanyuan Li, Email 15063102@163.com; liyy@outlook.com

Background: Ulcerative colitis (UC) is a debilitating inflammatory condition with growing global prevalence. While immune dysregulation is a known hallmark, the specific molecular drivers and their link to fibrosis remain incompletely characterized. To address this, we conducted a study combining bioinformatic analyses of public datasets with experimental validation to identify and validate key biomarker candidates involved in UC pathogenesis.

Methods: Three publicly available ulcerative colitis gene expression datasets (GSE38713, GSE87466, GSE119600) were retrieved from the Gene Expression Omnibus (GEO). Immune cell infiltration was evaluated using ssGSEA, with significant cell types identified by Wilcoxon test and LASSO regression. DEGs were screened and analyzed using GO, KEGG, and PPI networks. Hub genes were identified using cytoHubba and validated via ROC curves. RT-qPCR, WB, and IHC validated findings in UC rat models and clinical samples.

Results: The differentially expressed genes (DEGs) were evaluated using ten distinct algorithms, resulting in the identification of eight common DEGs following an intersection analysis. 4 hub genes were further identified through validation using the GSE119600 dataset, namely Cluster of Differentiation 274 (CD274), Matrix Metallopeptidase 1 (MMP1), neutrophil cytosolic factor 2 (NCF2), Plasminogen Activator Urokinase (PLAU). Notably, NCF2 demonstrated the highest specificity and sensitivity for diagnosing ulcerative colitis (UC), suggesting its potential utility as a diagnostic biomarker. Additionally, a distinct immune cell type exhibited significant differences between UC patients and healthy controls (HC). Correlation analyses utilizing bioinformatics techniques revealed that the hub genes CD274, MMP1, NCF2, and PLAU were positively associated with macrophage infiltration, highlighting their potential role in the immune response in UC.

Conclusion: CD274, MMP1, NCF2, PLAU can serve as hub genes associated with UC. Among these, NCF2 stands out as a particularly promising target for further research into the underlying mechanisms of UC. Additionally, NCF2 may play a role in the development and progression of UC by modulating macrophage infiltration.

Keywords: ulcerative colitis, differentially expressed genes, ssGSEA, immune cells, biomarker

Introduction

Ulcerative colitis (UC) is a chronic inflammatory bowel disease (IBD) characterized by inflammation localized to the colonic mucosa. The global prevalence of UC varies, with estimates ranging from 0.2% to 0.5% in Western populations, and there is a concerning increase in incidence in newly industrialized countries.[1,2] UC is a multifaceted disorder influenced by a combination of genetic predisposition, environmental factors, dysbiosis of gut microbiota, and abnormalities in immune system function.[3,4] Understanding these diverse influences is crucial for developing effective treatment strategies and improving patient outcomes.

Received: 9 July 2025
Accepted: 25 November 2025
Published: 3 December 2025

The pathogenesis of UC is primarily associated with dysregulated immune responses involving both innate and adaptive immunity. Patients often present with an overactive mucosal immune response, demonstrated by elevated levels of pro-inflammatory cytokines such as tumor necrosis factor-alpha (TNF-α) and interleukin-6 (IL-6). These cytokines are pivotal in driving inflammatory processes by facilitating the recruitment and activation of immune cells within the intestinal tract.[5] Moreover, interleukin-23 (IL-23) has emerged as a significant mediator that promotes the differentiation of T helper type 17 (Th17) cells, further exacerbating the inflammatory response.[6] A notable characteristic of UC is the impaired function of regulatory T cells (Tregs), which are essential for maintaining immune tolerance and controlling inflammation.[7]

Complications arising from UC include severe colitis, an increased risk of colorectal cancer, and potentially life-threatening conditions like toxic megacolon, which may necessitate surgical intervention.[8] Current treatment strategies focus on controlling inflammation through immunosuppressive agents and biologic therapies targeting specific inflammatory pathways. However, these approaches often fail to address the underlying mechanisms perpetuating chronic inflammation and tissue damage in UC.[9] While there is a recognized need to delineate the interactions among immune cells in UC pathophysiology, the roles of specific upstream regulators, particularly transcription factors like Nuclear Factor-C2 (NFC2), remain largely unexplored. Although implicated in immune regulation, the specific function and therapeutic potential of NFC2 in UC constitute a significant knowledge gap. To address this, our study employs an integrated bioinformatics approach (Figure 1) to test the hypothesis that NFC2 is a key regulator in UC. We aim to comprehensively analyze NFC2's expression, its associated pathways, and its interplay with the immune microenvironment, thereby evaluating its potential as a novel diagnostic biomarker and therapeutic target to improve clinical outcomes.

Materials and Methods

Data Source

Microarray data of intestinal mucosal tissues from UC patients and healthy controls were obtained from the GEO database (http://www.ncbi.nlm.nih.gov/geo/). The selection criteria for datasets included: (1) availability of mRNA expression profiles generated via microarray; (2) datasets containing both intestinal mucosa samples from UC patients and normal mucosal samples from healthy individuals; (3) inclusion of at least 30 samples per dataset; and (4) subjects aged 18 years or older. The final test datasets selected were GSE38713 and GSE87466, utilizing the GPL570 and GPL13158 platforms, respectively. The GPL10588 platform dataset GSE119600 was designated as the validation set.

A comprehensive analysis was conducted on a total of 43 biopsies, comprising 13 healthy controls, 8 inactive UC cases, 7 non-involved active UC cases, and 15 involved active UC cases. Specifically, the GSE38713 dataset included 30 UC patients, categorized as 8 with inactive disease, 7 with non-involved active disease, and 15 with involved active disease. The control group consisted of 13 healthy individuals with normal colon tissue. In the GSE87466 dataset, biopsies were collected from 87 UC patients and 21 healthy controls for RNA extraction and subsequent microarray analysis. The dataset (GSE119600) encompasses whole blood microarray data from 90 patients with primary biliary cholangitis (PBC), 45 with primary sclerosing cholangitis (PSC), 95 with Crohn's disease (CD), and 93 with UC, alongside 47 healthy controls. For further analysis, we focused on data from 93 UC patients and 47 healthy individuals. Table 1 offers an extensive overview of the four GSE datasets included in the study.

Data Preprocessing

The raw and series matrix files for GSE38713 and GSE87466 were downloaded for analysis. The probe expression matrices were extracted from the raw data and subsequently normalized using the "affy" R package (version 3.6.3). To convert the probe expression matrices into gene expression matrices, a platform annotation file was utilized. In instances where multiple probes corresponded to a single gene, the average expression value was calculated. Probes associated with multiple molecules were excluded from the dataset. The cleaned data sets were adjusted using the "ComBat" function from the "sva" R package. UMAP analysis was conducted to visualize the data, employing the "umap" R package, and graphical representations were created using the "ggplot2" R package.

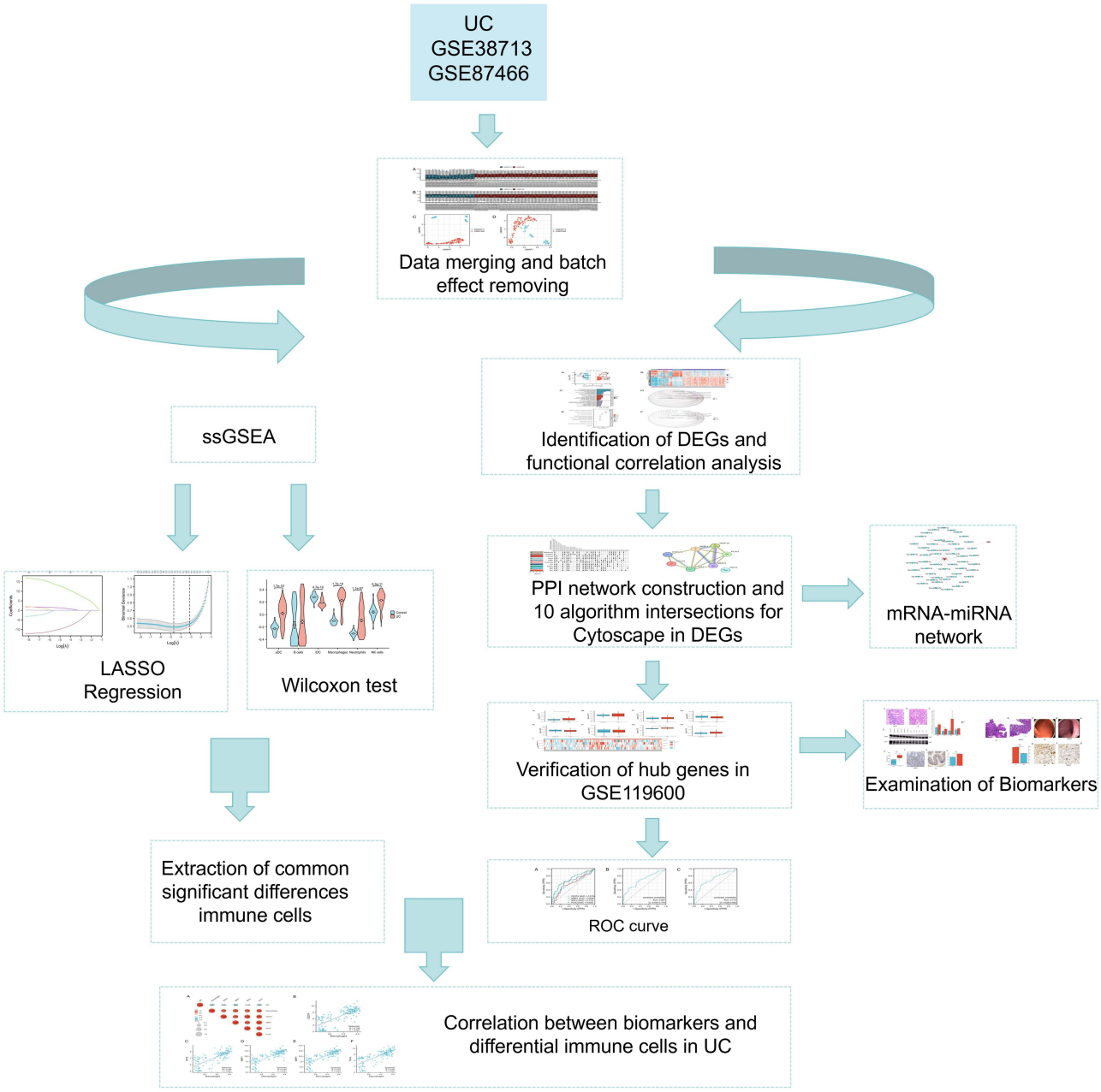

Figure 1 Flow chart of the analysis process conducted in this study.

Immune Cell Infiltration Analysis

The infiltration of immune cells in ulcerative colitis (UC) versus normal tissues was assessed using single-sample gene set enrichment analysis (ssGSEA). To identify significant differences in immune cell populations between the two groups, the Wilcoxon test and Least Absolute Shrinkage and Selection Operator (LASSO) regression analysis were employed. Specifically, five immune cell types were identified as significantly different by the Wilcoxon test, while LASSO regression highlighted two. The intersection of these analyses yielded two immune cell types that exhibited significant differences in infiltration ($p < 0.05$). The Wilcoxon test was performed using the wilcox.test function in R, and LASSO regression utilized the "glmnet" package. Visualization of the results was accomplished through the use of the "corplot," "vioplot," "ggplot2," and "glmnet" packages.

https://doi.org/10.2147/JIR.S552678

Table 1 Characteristics of the Included Datasets

Dataset ID	Country	Platforms	No. of Samples	Affymetrix GeneChip
GSE38713	Spain	GPL570	13 Healthy Control Samples 30 UC Patient Samples	Affymetrix Human Genome U133 Plus 2.0 Array
GSE87466	USA	GPL13158	21Healthy Control Samples 87 UC Patient Samples	Affymetrix HT HG-U133+ PM Array Plate
GSE119600	Poland	GPL10588	47 Healthy Control Samples 93 UC Patient Samples	Illumina HumanHT-12 V4.0 expression beadchip

Screening for Differential Genes and Functional Enrichment Analysis

Differential expression analysis of genes (DEGs) between UC samples and healthy controls was conducted using the R package "limma." Genes were identified as differentially expressed based on the criteria of $|\log2FC| > 1$ and p.adj < 0.05. For visualization, heatmaps and volcano plots were generated using the "ComplexHeatmap" and "ggplot2" packages, respectively. Functional enrichment analysis involved the conversion of gene identifiers through the "org.Hs.eg.db" package, followed by Gene Ontology (GO) and Kyoto Encyclopedia of Genes and Genomes (KEGG) pathway analyses using the "clusterProfiler" package. Significant pathways and functions were identified with thresholds set at p.adj < 0.05 and q-value < 0.2. The results of the enrichment analysis were also visualized utilizing the "ggplot2" package.

PPI Network Construction, Screening and Validation of Hub Genes

Protein-protein interaction (PPI) networks were established using all differentially expressed genes (DEGs) via the STRING online tool (https://string-db.org), applying stringent filtering criteria with a score threshold of >0.7. Interaction data files were then imported into Cytoscape (v3.9.1) for further analysis. Utilizing the top ten algorithms from cytoHubba—MCC (Maximum Clique Centrality), DMNC (Density of Maximum Neighborhood Component), MNC (Maximum Neighborhood Component), Degree, EPC (Edge Percolated Component), BottleNeck, EcCentricity, Closeness, Radiality, and Betweenness Centrality (BC)—the top 40 genes identified by each algorithm were selected. Gene screening was performed using the R package "UpSet." Key gene clusters were identified through Molecular Complex Detection (MCODE), with parameters set to a degree cutoff of 2, node score cutoff of 0.2, k-core of 2, max depth of 100. The three highest-scoring gene networks were chosen for visualization. Additionally, dataset GSE119600 was utilized for further validation to identify more robust hub genes.

Prediction of Targeting miRNAs

To investigate the roles of target genes and microRNAs (miRNAs), we performed a topological analysis and constructed gene-miRNA networks using miRTarBase v8.0 (https://miRTarBase.cuhk.edu.cn/). The interactions among hub genes and their corresponding miRNAs were subsequently visualized using Cytoscape, which allowed for a clearer understanding of their relationships.

Analyzing the Diagnostic Validity of Biomarkers

In the GSE119600 dataset, we developed logistic regression models utilizing the "glm" function from the R package. For receiver operating characteristic (ROC) analysis, the "pROC" package was employed, and visualizations were created using "ggplot2." The area under the curve (AUC) was computed to evaluate the diagnostic potential of UC biomarkers.

Correlation Analysis Between Hub Genes and Immune Cells

Using Spearman's rank correlation analysis in R software, we examined the correlation levels between four hub genes an two immune cells that are significantly elevated in UC, visualizing the results with the R package "ggplot2".

Animals

Twenty female wild-type C57BL/6 mice, aged 8–10 weeks and certified as specific pathogen-free (SPF), were obtained from the Yangzhou University Center for Comparative Medicine (Yangzhou, China) under license number YXYLL-2024-077. The animals underwent a minimum one-week acclimatization period with ad libitum access to food and water prior to the commencement of the experiment.

Establishment of DSS-Induced Colitis Model

C57BL/6 mice were randomly allocated into two groups: a control group (n = 6) and a DSS group (n = 6). Mice in the DSS group were administered drinking water containing 3.0% (w/v) dextran sulfate sodium (DSS, molecular weight 36–50 kDa, catalog number 60316ES60, YEASEN company) for a duration of 7 days. The control group received standard drinking water throughout the entire experimental period to mitigate potential confounding factors. Daily monitoring of body weight and assessment of colitis severity, including stool consistency, presence of blood in stool, and weight loss, was performed for each mouse. The disease activity index (DAI) was computed daily by amalgamating individual scores using a 0–4 scoring system based on the parameters delineated in Table 2. At the end of the experiment, mice were humanely euthanized via intraperit- oneal injection of a barbiturate-based anesthetic solution, following American Veterinary Medical Association (AVMA) guidelines.

UC and Control Samples from Patients

For this study, twelve formalin-fixed, paraffin-embedded tissue samples (six ulcerative colitis and six normal intestinal tissues) were obtained from the biobank at Yangzhou University Affiliated Hospital (Yangzhou, China). These samples were prospectively collected from consecutively enrolled patients between January 2022 and May 2024 under protocol #2022-YKL7, approved by the Institutional Review Board of Yangzhou University Affiliated Hospital (approval date: April 2021). All participants provided written informed consent for: Sample collection and storage in the biobank; Use of their de-identified samples in future research; Publication of aggregated data including individual patient details (No individually identifiable information is disclosed). The immunohistochemical analyses were performed in June 2024 following standard operating procedures.

Hematoxylin and Eosin (H&E) Staining

The tissue specimens were initially fixed in 10% buffered formalin for 48 hours at 4°C. Subsequently, they were embedded in paraffin and sectioned at a thickness of 4 μm. The slides then underwent dewaxing twice in 100% xylene for 30 minutes at 56°C and were rehydrated through a series of graded alcohol solutions (100%, 90%, 80%, 70%, and 50%). After a 5-minute rinse in H2O, the slides were stained with H&E (cat. no. G1121; Solarbio) for 10 minutes at room temperature. Following staining, the sections were serially dehydrated in ethanol, cleared in 100% xylene, and mounted with a coverslip using Permount (Wuhan Servicebio Technology Co., Ltd.) at room temperature. Finally, visualization of the sections was performed under a TE2000 microscope (Nikon Corporation of Japan) with white light.

RNA Isolation and Reverse Transcription-Quantitative PCR (RT-qPCR)

Tissue samples were homogenized with an ultrasonic cell disruptor (Branson, USA), and RNA was extracted using Trizol reagent (9112K1018; Takara Co., Ltd.). cDNA synthesis was performed using the Hifair® II 1st Strand cDNA Synthesis Kit (cat. no. 11121ES60, Yeasen Co., Ltd.) according to the manufacturer's protocol.

Table 2 Method for Calculating DAI

Score	Score 0	Score 1	Score 2	Score 3	Score 4
Weight Loss	No apparent decrease <5%	Slight decrease (1%–5%)	Moderate decrease (5%–10%)	Marked decrease (10%–20%)	Severe decrease (>20%)
Stool Consistency	Normal	Slightly soft	Mucoid	Watery	Bloody
Rectal Bleeding	None	Slight (light blue)	Mild (blue)	Severe (dark blue)	Gross visible blood

Notes: DAI = Score for Weight Loss + Score for Stool Consistency + Score for Rectal Bleeding.

Quantitative polymerase chain reaction (qPCR) was conducted with the Hieff® qPCR SYBR Green Master Mix (NoRox) kit (cat. no. 11201ES03, Yeasen). The thermal cycling conditions included initial denaturation at 94°C for 3 minutes, followed by 40 cycles of 94°C for 10 seconds and 60°C for 30 seconds. Data from three independent experiments were analyzed using the 2-ΔΔCq method, with glyceraldehyde 3-phosphate dehydrogenase (GAPDH) as the internal control. Primer sequences are listed in Table 3.

Western Blotting and Antibodies

Tissue samples were processed using qPCR methodology. Homogenized tissue was lysed with RIPA Lysis Buffer (with PMSF) on ice, and protein concentration was measured using a BCA Protein Assay Kit. Twenty micrograms of protein were mixed with loading buffer, heated at 95°C, and separated by 10% SDS-PAGE at 120 V for 1.5 hours. Proteins were transferred to 0.22-μm PVDF membranes. Membranes were blocked with 5% skimmed milk in TBST for 1 hour, then incubated overnight with primary antibodies at 4°C. After washing, membranes were treated with HRP-conjugated Goat Anti-Rabbit IgG and bands were visualized using an ECL kit. Primary antibodies included β-actin (1:3,000) and anti-NCF2 (1:2,000). Semi-quantitative analysis was done using ImageJ software.

Immunohistochemical Staining

Immunohistochemical analysis was performed to assess NCF2 expression in colon and rectal tissues. Paraffin sections (5 μm) were deparaffinized using xylene and rehydrated through graded ethanol. The sections were treated with 3% hydrogen peroxide for 15 minutes to block endogenous peroxidase activity, followed by blocking with goat serum for 30 minutes at room temperature. Next, the sections were incubated overnight at 4°C with primary antibodies against NCF2 (Sanying, Wuhan, China). The following day, detection was carried out using an immunohistochemistry kit (KIT-9720, MXB), followed by incubation with HRP-conjugated secondary antibodies for 30 minutes at 37°C. Visualization was achieved with DAB chromogen, and hematoxylin was used for counterstaining. Images were captured using the BioTek Cytation 5 (BioTek, USA), and the percentage area of positive staining was quantified with ImageJ software.

Statistical Analysis

Statistical analyses were conducted using R software (version 4.1.2), SPSS 26.0 (IBM Corp)., and Prism 8 (Dotmatics). For the qPCR experiments, data were assessed using the unpaired Student's *t*-test. Similarly, the unpaired Student's *t*-test was employed for data analysis in the Western blot and immunohistochemistry experiments. Each experiment was independently repeated three times to confirm reproducibility. A significance threshold of $P < 0.05$ was established to determine statistical significance.

Results

Immune Infiltration ssGSEA Analysis

We utilized two microarray datasets: GSE38713 from the GPL570 platform and GSE87466 from the GPL13158 platform, encompassing a total of 117 ulcerative colitis (UC) samples and 34 normal samples. The data before batch correction (Figure 2A and B) exhibited significant batch effects; however, post-batch correction (Figure 2C and D), these discrepancies were effectively mitigated, resulting in well-normalized data.

Table 3 Primer Sequences

Gene	Primer Sequence (F)	Primer Sequence (R)
NCF2	GGAGAAGTACGACCTTGCTATCA	ACAGGCAAACAGCTTGAACTG
CD274	GCTCCAAAGGACTTGTACGTG	TGATCTGAAGGGCAGCATTTC
PLAU	ATGGAAATGGTGACTCTTACCGA	TGGGCATTGTAGGGTTTCTGA
MMP1	CCTTGATGAGACGTGGACCAA	ATGTGGTGTTGTTGCACCTGT

Abbreviations: F, forward; R, reverse.

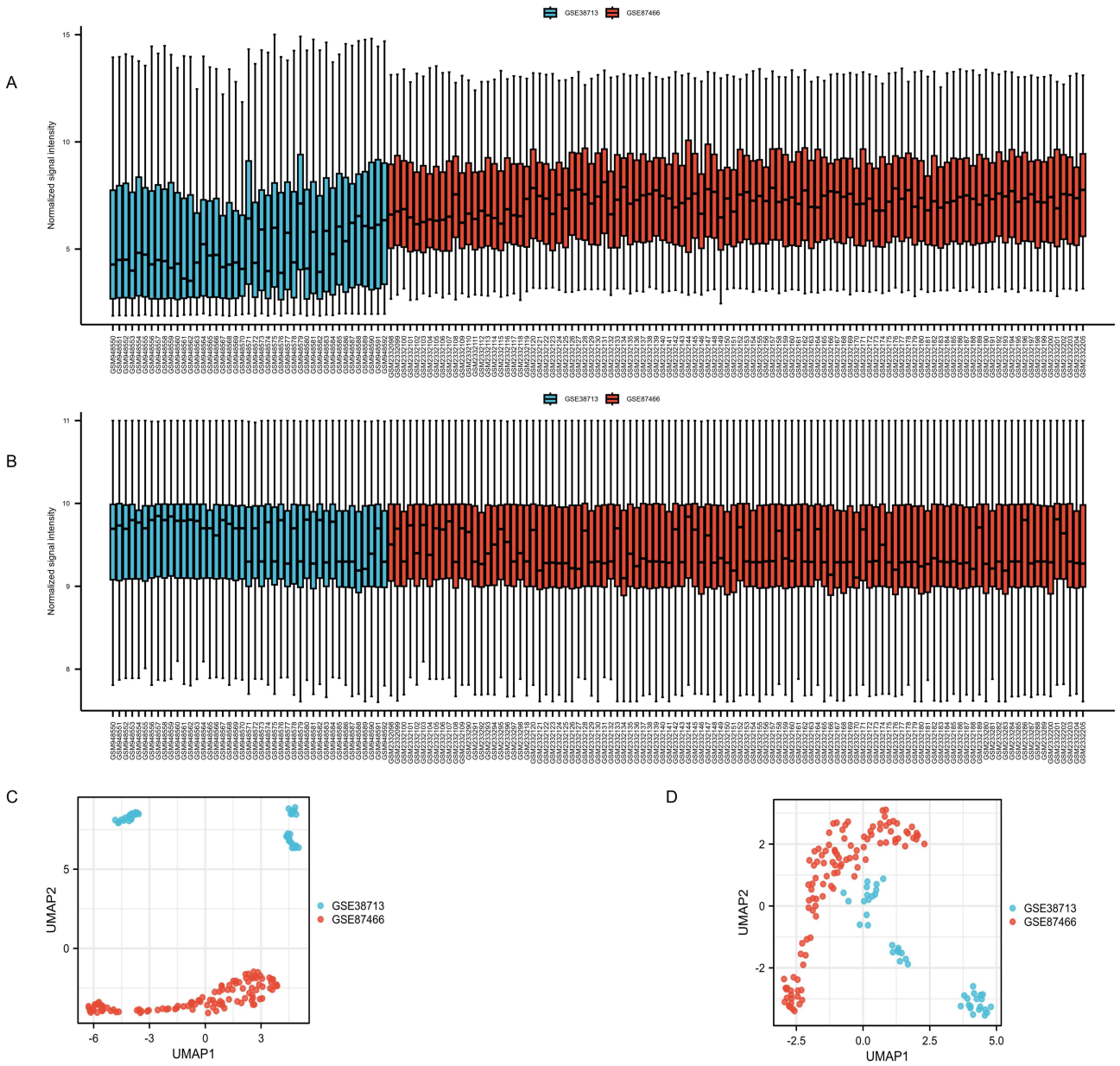

Figure 2 Data preprocessing. Box plot and uniform manifold approximation projection (UMAP) were applied to correct for batch effects in the GSE38713 and GSE87466 datasets. (**A** and **B**) before batch correction and (**C** and **D**) after batch correction.

To assess immune cell correlations within each sample, we presented the findings in a heat map format (Figure 3A). We employed two distinct statistical approaches—Wilcoxon test and LASSO regression—to identify significant variations in immune cell infiltration between UC and normal samples. The results derived from the Wilcoxon test are illustrated in a violin plot (Figure 3B), highlighting five immune cells with $p<0.05$. Furthermore, the LASSO regression analysis (Figure 3C and D) identified two immune cells of interest. Notably, two immune cells, immature dendritic cells (iDC) and macrophages, were consistently identified by both methodologies.

Screening for Differential Genes and Associated Functional Analysis

In UC samples, we identified 150 differentially expressed genes (DEGs) when compared to normal controls, including 90 genes with increased expression and 60 genes with decreased expression. Visualization of these DEGs was performed through heat maps and volcano plots, as shown in Figure 4A and B. Gene Ontology (GO) analysis indicated that the

https://doi.org/10.2147/JIR.S552678

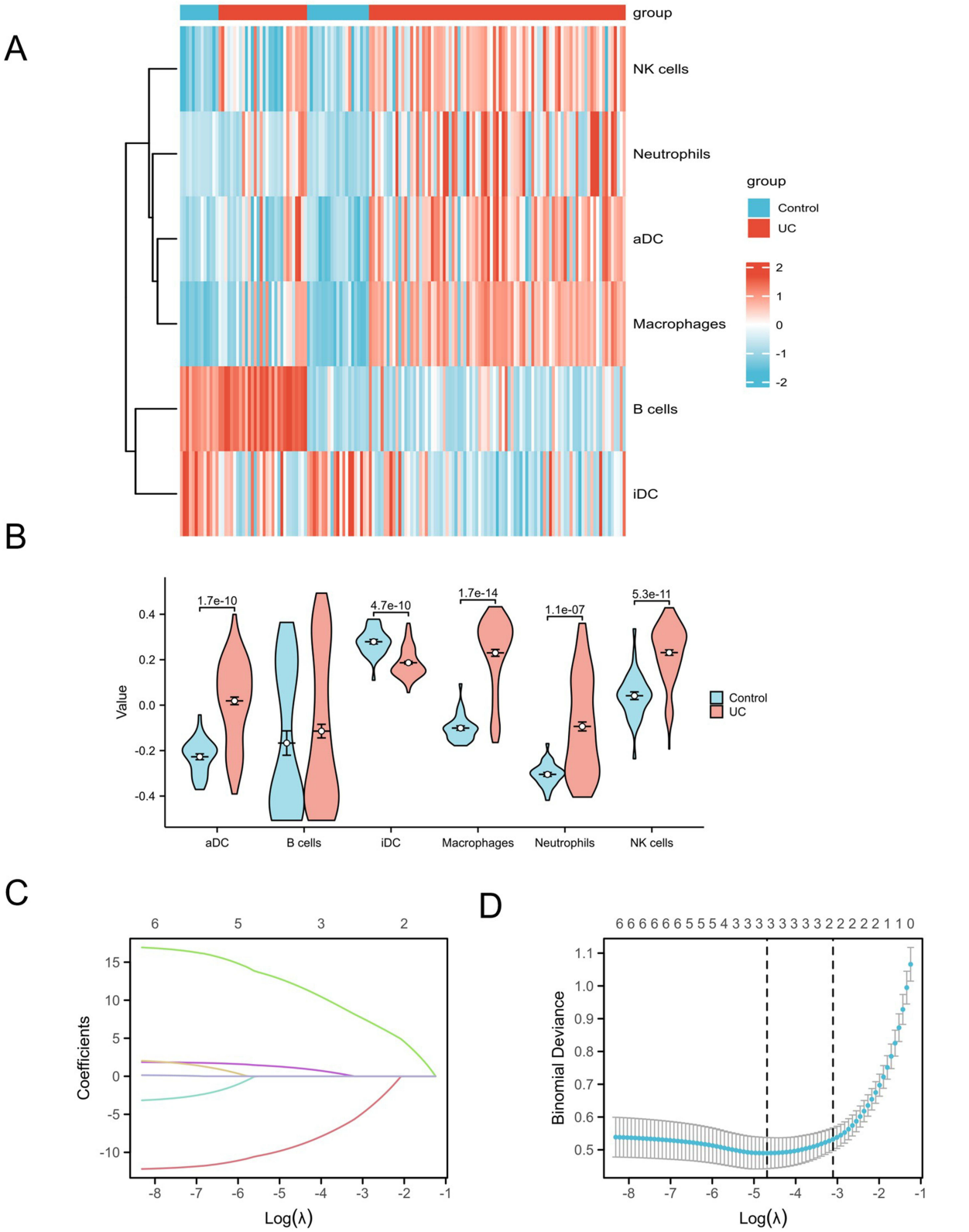

Figure 3 Immune cell infiltration was analyzed to identify significant differences in immune cell populations between CD and normal tissues. The relative abundance of 7 immune cell types across samples is presented in a heatmap (**A**). Statistical analysis was performed using the Wilcoxon test (**B**), and LASSO regression (**C** and **D**) was employed to assess the variations in immune cell infiltration.

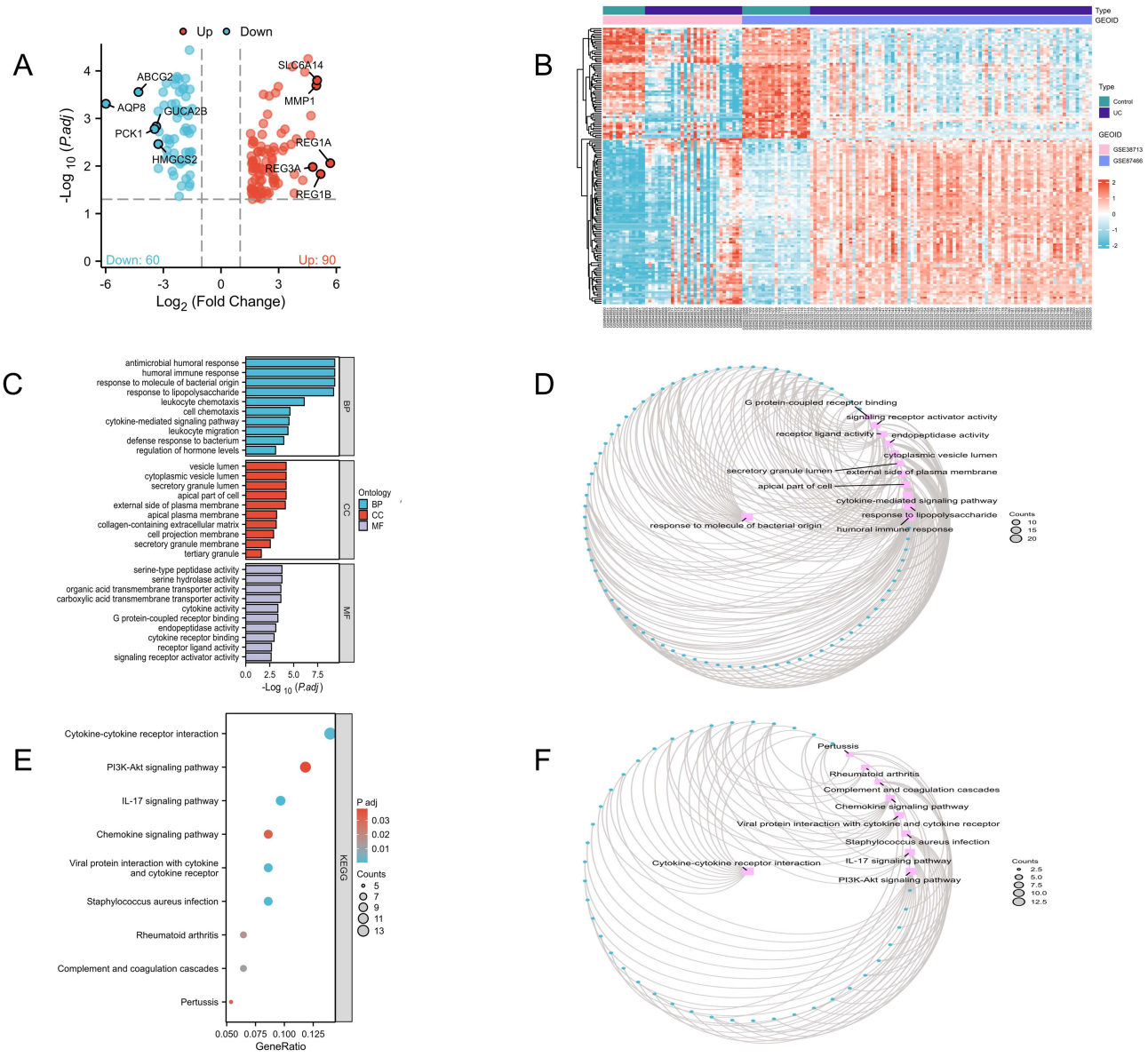

Figure 4 DEGs were identified, and functional enrichment analysis was performed using GO and KEGG. The DEGs are illustrated in a volcano plot (**A**) and heatmap (**B**). GO enrichment results are displayed in a bar plot (**C**) and circle plot (**D**), while KEGG pathway analysis is shown in a bubble plot (**E**) and circle plot (**F**).

DEGs were primarily enriched in biological processes related to immune responses, such as antimicrobial humoral response, humoral immune response, response to bacterial molecules, and leukocyte chemotaxis. Key cellular components included vesicle lumen, cytoplasmic vesicle lumen, and secretory granule lumen. Molecular functions predominantly involved serine-type peptidase activity and cytokine activity. The top ten enriched terms were selected based on a significance threshold of p.adj < 0.05, shown in a bar graph. The top five entries for each category of biological processes, cellular components, and molecular functions were visualized in a circular graph (Figure 4C and D).

KEGG pathway enrichment analysis revealed that the DEGs were closely linked to immune and inflammatory signaling pathways, particularly the cytokine-cytokine receptor interaction pathway, IL-17 signaling pathway, and chemokine signaling pathway. Other significant pathways included the PI3K-Akt signaling pathway and viral protein interactions with cytokines and their receptors. A total of nine KEGG pathways were selected based on the p.adj < 0.05 threshold, illustrated through bubble and network diagrams (Figure 4E and F).

https://doi.org/10.2147/JIR.S552678

Identification and Validation of Hub Genes

The protein-protein interaction (PPI) network for differentially expressed genes (DEGs) was constructed using the STRING database, resulting in 111 nodes and 389 edges. Unconnected nodes were removed for clearer visualization (Figure 5A). Next, data were analyzed in Cytoscape, where node sizes were adjusted based on betweenness centrality (BC) values (Figure 5B). The MCODE plugin identified three significant gene clusters: Cluster 1 (score: 8.6, 11 nodes, 43 edges), Cluster 2 (score: 4.6, 11 nodes, 23 edges), and Cluster 3 (score: 4.5, 5 nodes, 9 edges) Cluster 4 (score: 4, 4 nodes, 6 edges) (Figure 5C–F).

To identify key DEGs, the top 40 genes from each of 10 algorithms were analyzed using the R package "UpSet," revealing eight critical DEGs: CD274, CXCL1, CXCL11, MMP1, MMP10, MMP3, NCF2, and PLAU (Figure 6A). These genes were visualized in the PPI network (Figure 6B). Additionally, a co-expression network linking mRNA and miRNA was created in Cytoscape, comprising 2 genes, 51 nodes, and 50 edges (Figure 6C). Validation using the GSE119600 dataset indicated that NCF2, CD274, PLAU, and MMP1 had significantly higher expression in ulcerative colitis (UC) samples compared to healthy controls ($p < 0.01$). These genes were designated as hub genes related to UC, with expression differences shown in a heatmap (Figure 7).

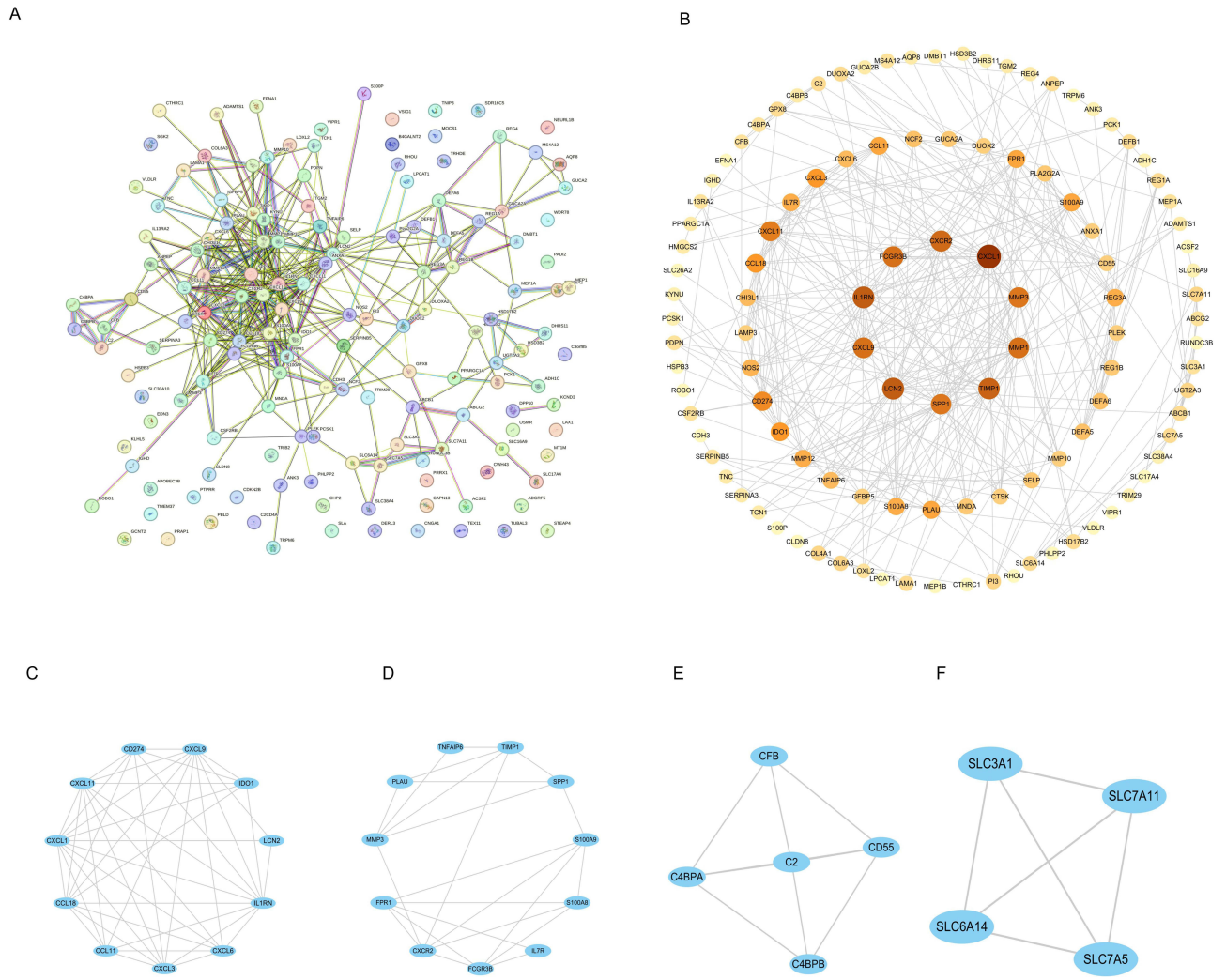

Figure 5 PPI network and clustering analysis. The PPI network was generated using the STRING database, with edges representing both functional and physical protein interactions (**A**). The PPI network was visualized and optimized using Cytoscape software, with node color intensity reflecting the degree of differential expression (**B**). The four most significant gene cluster modules were identified from the PPI network using the Molecular Complex Detection (MCODE) algorithm, with each module representing a highly interconnected protein complex. Nodes are colored by cluster membership, and node size corresponds to the degree of connectivity within each module (**C**–**F**).

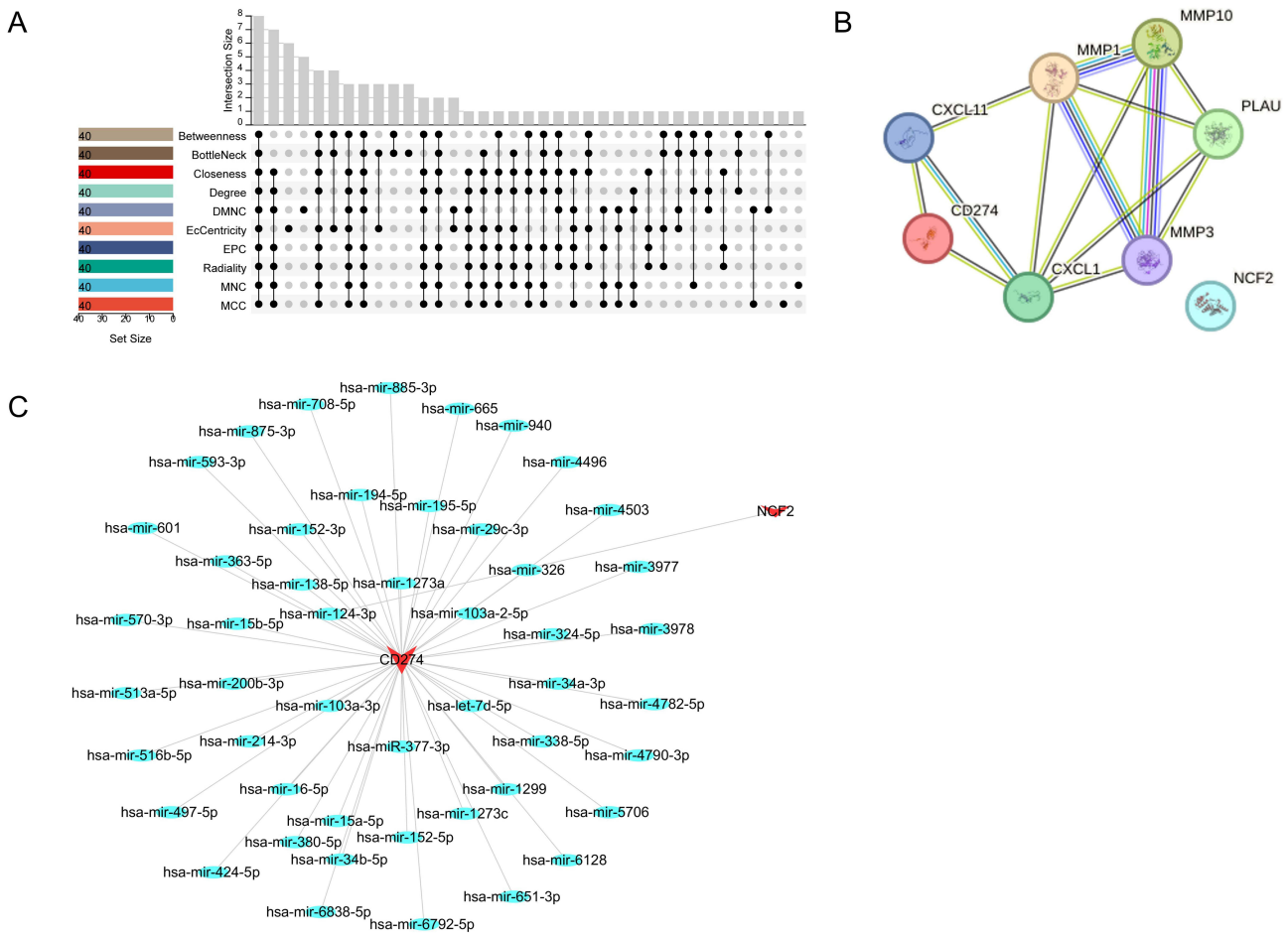

Figure 6 Identification of hub genes and the mRNA-miRNA co-expression network. Hub genes were selected using the R package "Upset" (**A**). The interaction degree of the 9 hub genes was visualized with STRING software (**B**). The mRNA-miRNA co-expression network, comprising 51 nodes and 50 edges, was constructed and visualized using Cytoscape (**C**).

Screening Biomarkers for UC

The diagnostic efficacy of CD274, MMP1, NCF2, and PLAU for UC was assessed using receiver operating characteristic (ROC) analysis with the GSE119600 dataset. An area under the curve (AUC) closer to 1 indicates better diagnostic performance. Among the markers, NCF2 showed the highest predictive accuracy with an AUC of 0.715 (95% confidence interval [CI] = 0.628–0.802), followed by PLAU at 0.625 (95% CI = 0.527–0.722) and CD274 at 0.615 (95% CI = 0.522–0.709). MMP1 had the lowest accuracy with an AUC of 0.608 (95% CI = 0.510–0.707) (Figure 8A).

When analyzing gene combinations, NCF2 and PLAU together yielded a combined AUC of 0.715 (95% CI = 0.628–0.802), while NCF2 and CD274 produced an AUC of 0.687 (95% CI = 0.597–0.776) (Figure 8B and C). Thus, NCF2 demonstrated the highest sensitivity and specificity among individual biomarkers, with the combination of NCF2 and PLAU offering optimal specificity.

Correlation Analysis Between Hub Genes and Immune Cells

Four biomarkers (CD274, MMP1, NCF2, PLAU) were analyzed for their correlation with two immune cell types (iDC, Macrophages) using the Wilcoxon test and LASSO regression analysis. Correlation assessments were conducted, and significant relationships were identified with a correlation coefficient (R) of ≥0.75 and a p-value <0.001 (Figure 9A). The analysis revealed that Macrophages exhibited positive correlations with CD274 (R=0.746, p<0.001), MMP1 (R=0.797, p<0.001), NCF2 (R=0.765, p<0.001), and PLAU (R=0.797, p<0.001) (Figure 9B–E).

https://doi.org/10.2147/JIR.S552678

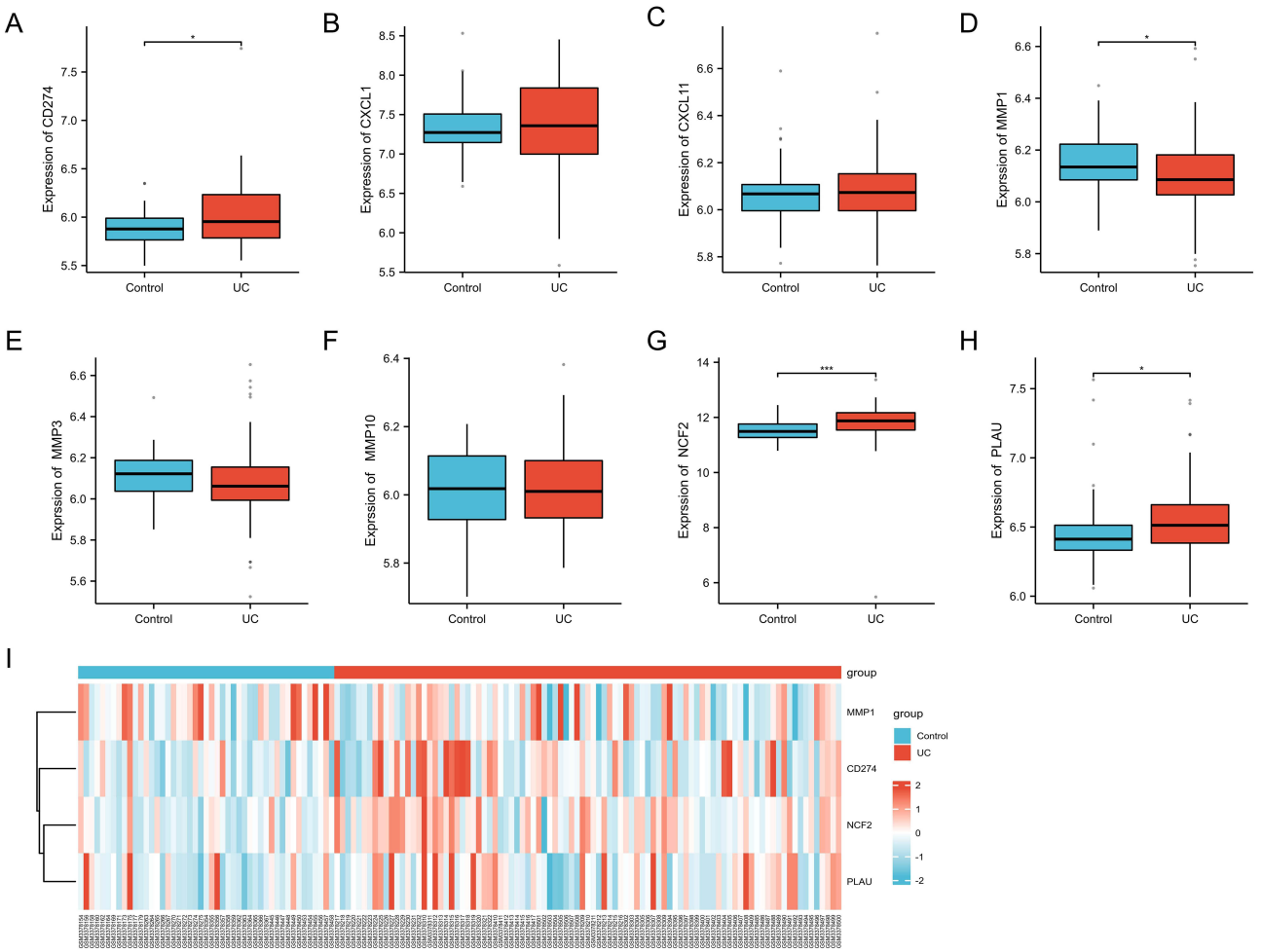

Figure 7 Validation of hub genes. The expression of 8 hub genes was assessed using the GSE119600 dataset. NCF2 expression was significantly higher in UC and active UC samples compared to HC ($p < 0.001$), while CD274, PLAU, and MMP1 were upregulated in active UC relative to HC ($p < 0.05$) (**A**–**H**). A heatmap showing the expression levels of CD274, MMP1, NCF2, and PLAU is provided (**I**). (*$p < 0.05$, ***$p < 0.001$).

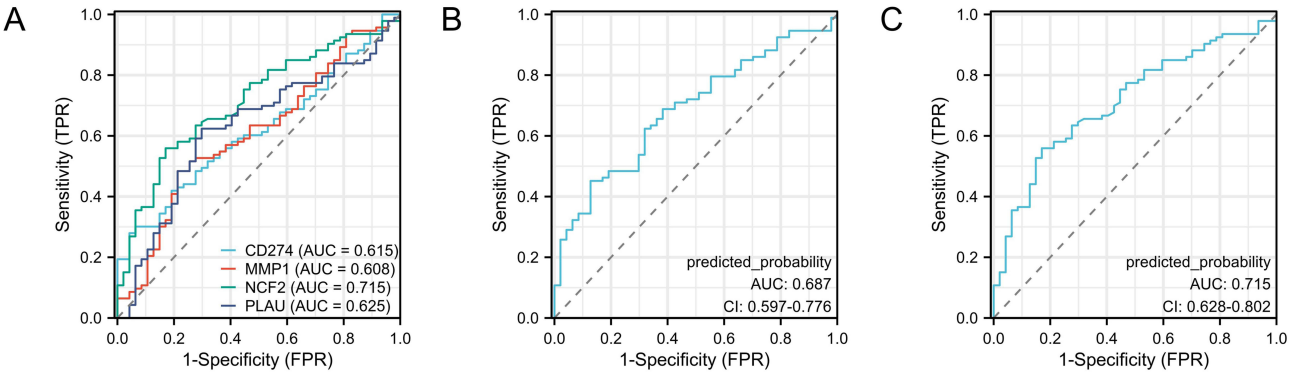

Figure 8 ROC curves of the 4 specifically expressed hub genes. Diagnostic value of CD274, MMP1, NCF2 and PLAU in UC using non-inflammatory tissues as controls by dataset GSE119600 (**A**). Diagnostic value of NCF2 and PLAU in UC (GSE119600 dataset) (**B**). Diagnostic value of NCF2 and CD274 in UC (GSE119600 dataset) (**C**).

Examination of Biomarkers in Animal Models of UC and UC Clinical Samples

To further assess the expression of CD274, MMP1, NCF2, and PLAU in ulcerative colitis (UC), a rat model was induced using dextran sulfate sodium (DSS). Histological analysis via H&E staining revealed well-preserved colonic architecture in the control group, with intact mucosal layers and no evidence of ulceration or hyperplasia. In contrast, the DSS-treated

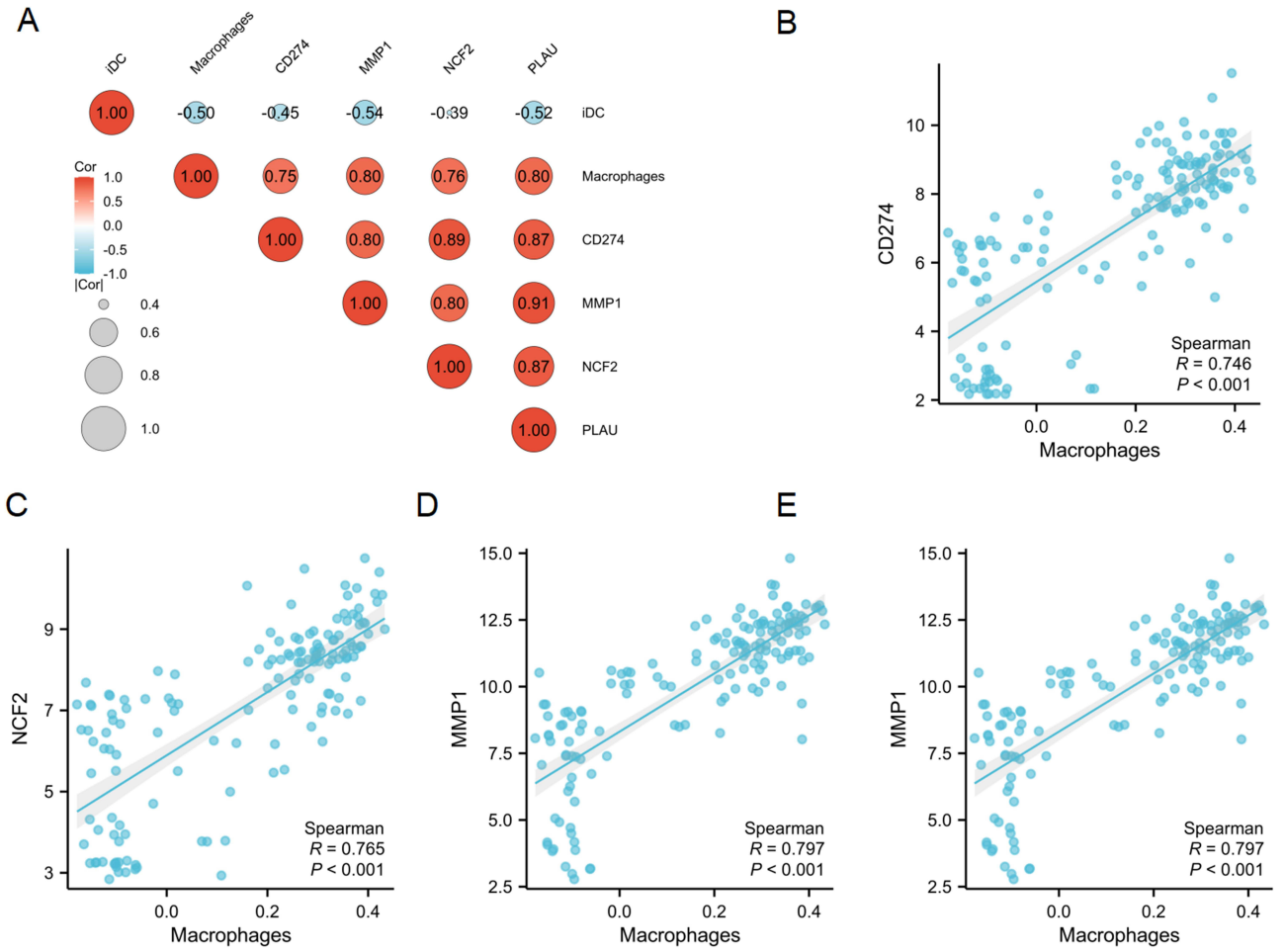

Figure 9 Correlation between hub genes and differential immune cells in UC. Correlation of 4 hub genes and 2 significantly differential immune cells (**A**). CD274, MMP1, NCF2, PLAU were positively correlated with Macrophages (**B**–**E**).

model group exhibited significant inflammatory cell infiltration, disruption of tissue structure, glandular destruction, and ulcerations (Figure 10A and B).

Gene expression analysis revealed a marked upregulation of NCF2, whereas CD274, MMP1, and PLAU demonstrated stable expression levels with no significant differences observed (Figure 10C). Western blotting further validated these findings, showing a significant increase in NCF2 protein levels in DSS-induced UC tissues compared to controls ($P<0.05$) (Figure 10D and E). Immunohistochemical staining confirmed heightened expression of NCF2 in the colonic tissues of DSS-treated rats, supporting its potential role in UC pathogenesis (Figure 10F–H).

In clinical UC samples, tissue specimens were confirmed by two independent pathologists following colonoscopy, tissue sectioning, and H&E staining, with detailed clinicopathological information summarized in Table 4. Colonoscopic findings (Figure 11A and B) and H&E staining (Figure 11C and D) showed substantial inflammatory cell infiltration and lymphocyte accumulation in the intestinal mucosa of UC patients. Immunohistochemical analysis of NCF2 expression in both normal and UC tissues (Figure 11E–G) corroborated results from the mouse model, aligning with qPCR and Western blot data.

Discussion

Ulcerative colitis (UC) is a chronic inflammatory bowel disease characterized by persistent mucosal inflammation, primarily affecting the colon. The pathophysiology of UC is complex and involves a multifactorial interplay of immune system dysregulation, genetic predisposition, and environmental triggers.[9] The dynamics of immune cell populations are

https://doi.org/10.2147/JIR.S552678

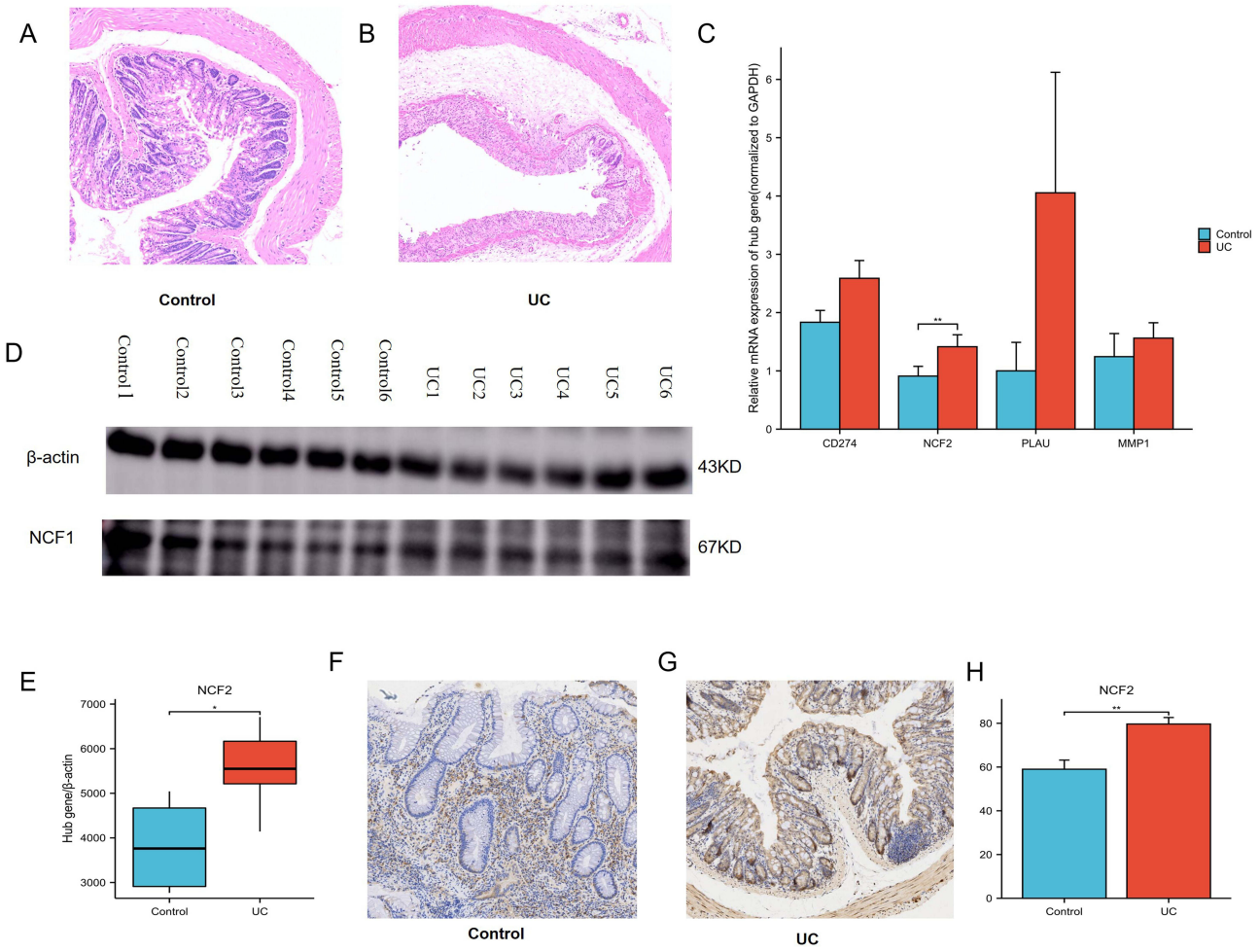

Figure 10 Examination of biomarkers in animal models of UC. Hematoxylin and eosin (H&E)-stained images of normal mouse colon tissue, scale bar,100μm (**A**); H&E-stained images of colon tissue from dextran sulfate sodium (DSS)-induced colitis mice, scale bar,100μm (**B**); Bar graph comparing the expression levels of hub genes in the intestines of normal and UC mice, as determined by RT-qPCR (**C**); Western blot analysis of NCF2 protein expression in the intestines of normal and UC mice (**D**); Box plot showing NCF2 protein expression levels in the normal and UC groups (**E**); Immunohistochemical staining of NCF2 protein in normal mouse colon tissue, scale bar,20μm (**F**); Immunohistochemical staining of NCF2 protein in UC mouse colon tissue, scale bar,20μm (**G**). Box plot comparing NCF2 protein expression levels in the normal and UC groups based on immunohistochemical analysis (**H**). (*P<0.05,**P<0.01,***P<0.001).

critical in the progression of UC; increased pro-inflammatory cytokines and immune cell infiltration in affected tissues are well-documented factors that contribute to ongoing inflammation and tissue injury.[3,10] These insights suggest the potential for targeted immunotherapies designed to restore immune balance and alleviate inflammation. Moreover, identifying novel biomarkers associated with immune dysregulation may enhance our understanding of the disease mechanisms and lead to improved therapeutic strategies.[11] In this study, we utilized advanced bioinformatics techniques to explore the immune cell landscape in UC tissues compared to healthy controls. Our goal was to uncover reliable biomarkers that could inform treatment approaches and enhance patient management in UC. These findings aim to further elucidate the intricate immune interactions in UC and contribute to the development of more effective therapeutic interventions.

The intestinal tissues of UC patients exhibited notable differences in the distribution of macrophages and immature dendritic cells (iDCs) when compared to normal tissues. Macrophages, as key regulators of organ function, play essential roles in both tissue homeostasis and response to injury. They originate from embryo-derived progenitors and are tissue-resident cells that maintain close relationships with other specialized tissue cells. These macrophages contribute to various physiological processes, including tissue growth, regeneration, and defense against disease.[12] However, following organ injury, macrophages undergo significant changes in phenotype and function, which can drive maladaptive repair processes, leading to chronic inflammation and fibrosis.[13] Macrophages play a crucial role in UC by mediating inflammation, tissue healing, and

Table 4 Clinicopathological Characteristics of Patients with UC's Disease

Characteristic	Age, Years	Sex	Sample Location
UC Patient 1	53	Female	Sigmoid colon
UC Patient 2	64	Female	Sigmoid colon
UC Patient 3	41	Male	Rectum
UC Patient 4	52	Male	Rectum
UC Patient 5	44	Male	Sigmoid colon
UC Patient 6	60	Female	Rectum
Control 1	42	Male	Sigmoid colon
Control 2	33	Male	Rectum
Control 3	56	Female	Sigmoid colon
Control 4	33	Female	Sigmoid colon
Control 5	41	Male	Rectum
Control 6	60	Female	Rectum

host defense through the production of cytokines, chemokines, and phagocytosis, while maintaining immune tolerance to the intestinal microbiota.[14,15] Immature dendritic cells (DCs) are typically circular in shape, have low expression of costimulatory molecules, and exhibit strong phagocytic activity, playing a crucial role in initiating the immune response. As they mature, DCs develop longer dendrites and increase their expression of costimulatory molecules.[16] In ulcerative colitis (UC), immature DCs are more abundant in the colonic mucosa and function as antigen-presenting cells, contributing to immune activation and inflammation. Additionally, these DCs are involved in neurotransmitter release and interact with gut enterochromaffin cells and autonomic nerves, further promoting intestinal inflammation.[17]

Our network analysis identified hsa-mir-124-3p as a top-ranked miRNA with predicted regulatory interactions of key hub genes, including NCF2. This computational prediction is strongly supported by emerging evidence that positions

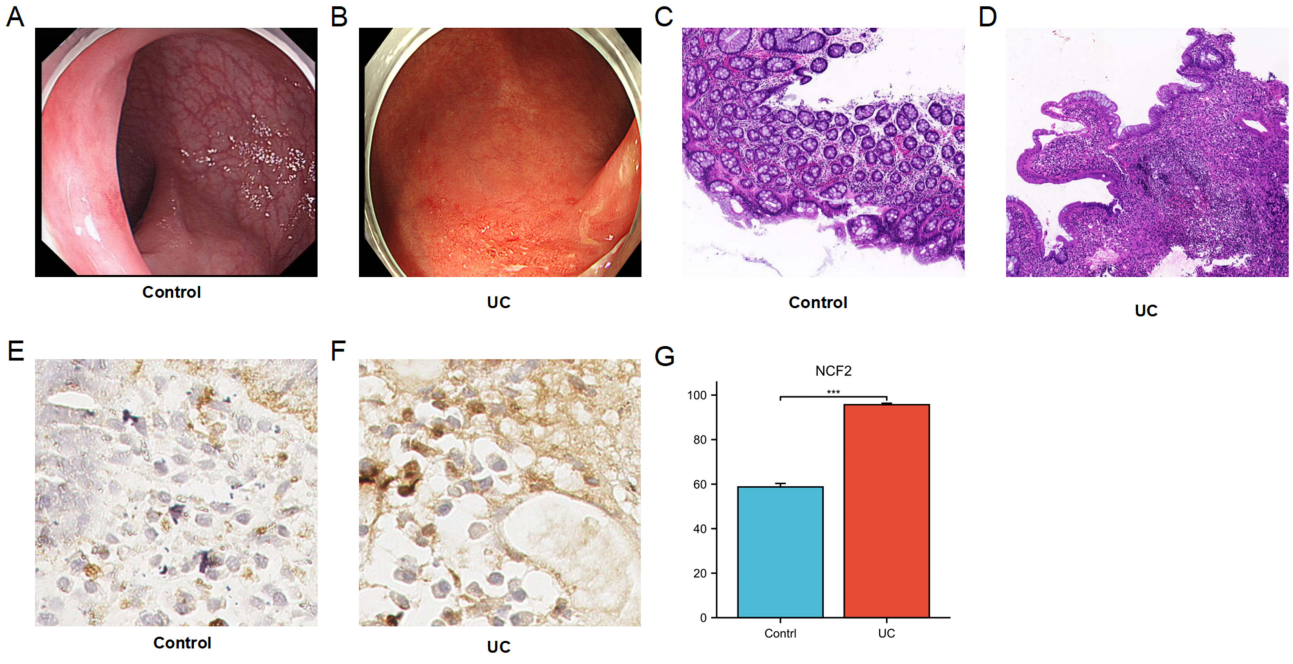

Figure 11 Examination of biomarkers in UC clinical samples. Representative colonoscopic findings of normal intestinal mucosa (**A**); Colonoscopic appearance of intestinal mucosa in patients with ulcerative colitis (**B**); Hematoxylin and eosin (H&E)-stained histological sections of normal intestinal mucosa, scale bar = 100 μm (**C**); H&E-stained histological sections of intestinal mucosa from UC patients, scale bar = 100 μm (**D**); Immunohistochemical staining showing NCF2 expression in colonic tissue from normal subjects, scale bar = 20 μm (**E**); Immunohistochemical staining showing NCF2 expression in colonic tissue from UC patients, scale bar = 20 μm (**F**); Bar graph comparing the immunohistochemical expression levels of NCF2 between normal and UC intestinal tissues (**G**) ***P < 0.001.

https://doi.org/10.2147/JIR.S552678

miR-124 as a critical modulator of inflammation in ulcerative colitis (UC). Notably, the therapeutic agent ABX464, which selectively upregulates miR-124, has been shown to act as a "physiological brake" on inflammation in UC by suppressing pro-inflammatory pathways such as the IL-17/Th17 axis, a effect demonstrated across in vitro, murine, and human studies.[18] This mechanism underlies the observed reduction in inflammatory cytokines and is associated with the rapid, sustained efficacy and favorable safety profile of ABX464. The prediction that miR-124 interacts with NCF2 suggests a novel, specific mechanism through which it may suppress ROS production and macrophage activation, thereby adding a crucial dimension to its known anti-inflammatory role. To fully realize the precision medicine potential of these findings, future work must prioritize the experimental validation of the miR-124-NCF2 interaction and investigate its relevance across different UC disease endotypes.

After confirming eight differentially expressed genes, the reliability of the GSE119600 dataset was reassessed, ultimately identifying four hub genes for ulcerative colitis: CD274, MMP1, NCF2, and PLAU. CD274 (PD-L1) plays a crucial role in immune regulation by inhibiting T-cell activation, and its expression may influence inflammatory responses in ulcerative colitis (UC).[19] MMP1 (Matrix Metalloproteinase-1) is involved in extracellular matrix remodeling and contributes to tissue repair and inflammation, making it relevant to the pathology of UC.[20] ROC regression analysis indicated that the combination of NCF2 and PLAU demonstrated the highest sensitivity and specificity for diagnosing UC. The role of NCF2 in immune response and inflammation is intricately tied to its function within the NADPH oxidase complex, which is essential for phagocytic cell activation and microbial killing.[21] NCF2 encodes the cytosolic subunit p67phox, and mutations in this gene are associated with several immune and inflammatory disorders, including chronic granulomatous disease (CGD) and autoimmune diseases.[21,22] PLAU is a key mediator of immune responses and inflammation in cancer. Its expression influences tumor progression through immune cell recruitment, inflammation, and ECM remodeling.[23,24]

Importantly, while these hub genes were initially identified from intestinal tissue microarray data, they also demonstrated robust diagnostic value in validation using blood transcriptome datasets. This intriguing observation suggests that the dysregulation of these genes is not confined to the local intestinal environment but reflects a systemic alteration in circulating immune cells. This systemic signature may be attributed to the recirculation of activated immune cells between the gut and peripheral blood, as well as the dissemination of inflammatory mediators from the site of mucosal inflammation into the systemic circulation. The fact that these biomarkers are detectable in blood significantly enhances their clinical translatability, offering a less invasive means for disease diagnosis and monitoring. This finding underscores the profound interconnection between local intestinal inflammation and systemic immune responses in UC, positioning CD274, MMP1, NCF2, and PLAU as promising and versatile biomarkers indicative of the disease's systemic footprint.

The interplay between immature dendritic cells (iDCs) and macrophages is pivotal in the pathogenesis of ulcerative colitis (UC). This interaction significantly influences the inflammatory processes that characterize the disease. Immature dendritic cells (iDCs) serve as essential antigen-presenting cells that play a crucial role in maintaining immune tolerance within the intestinal mucosa. The activation and maturation of immature dendritic cells (iDCs) in ulcerative colitis (UC) can lead to an amplified immune response, facilitating the activation of T cells, particularly the Th1 and Th17 subsets, which are closely linked to the inflammatory processes observed in the disease.[25–27] Macrophages frequently exhibit a pro-inflammatory M1 phenotype, which exacerbates the condition through the secretion of cytokines such as TNF-α and IL-1β, as well as reactive oxygen species (ROS). This secretion contributes to epithelial barrier dysfunction and perpetuates the inflammatory cycle.[28,29] Moreover, macrophages can modulate the activity of immature dendritic cells (iDCs) and other immune cells, thereby enhancing the overall immune response.[30,31] This complex interplay highlights the potential for targeting these immune cell populations in therapeutic approaches for UC.

Considering the strong connection between immune infiltrating cells and hub genes in UC we examined the correlation between significantly different immune cells and the hub gene. The present findings reveal a positive correlation between NCF2 and macrophages, alongside a negative correlation with immature dendritic cells (iDCs). This suggests that NCF2 may play a crucial role in the activation and functional modulation of macrophages within the inflammatory milieu of ulcerative colitis (UC). Macrophages are integral to the inflammatory response, and their activation can significantly contribute to tissue damage observed in UC. NCF2 regulates reactive oxygen species (ROS) production via NADPH oxidase, influencing both innate and adaptive immunity,[32] and exacerbating inflammation in UC.[33] Pterostilbene-based nanoparticles could offer therapeutic potential by modulating ROS levels, specifically

targeting macrophage polarization and cytokine release.[34] NCF2 is essential for ROS-mediated LC3-associated phagocytosis (LAP) in macrophages against Listeria monocytogenes, whereas the pore-forming toxin-induced PINCA pathway, although activated in its absence, does not effectively contribute to bacterial clearance.[35]

Conversely, the negative correlation between NCF2 and iDCs implies that NCF2 may influence the differentiation or functional capacity of these cells. IDCs are essential for effective antigen presentation and the initiation of adaptive immune responses.[36] Therefore, reduced expression of NCF2 could impair their function, potentially resulting in inadequate immune responses in patients with UC. In summary, NCF2 may influence macrophages and iDCs to regulate both innate and adaptive immune responses, ultimately worsening the intestinal inflammatory reaction.

A significant proportion of patients with ulcerative colitis (UC) will experience recurrent disease flares, leading to chronic inflammation and progressive mucosal damage.[37] Over time, the continuous inflammatory cycle results in ulceration, excessive extracellular matrix (ECM) deposition, and localized fibrosis within the mucosa and submucosa.[38] Although UC predominantly affects the superficial layers of the colon, persistent tissue repair and collagen accumulation can contribute to complications such as bowel strictures, toxic megacolon, and in some cases, colorectal cancer. These complications often require surgical intervention, including colectomy, especially in cases of refractory disease or severe disease relapse.[39–41] Identifying biomarkers that can predict disease progression and the likelihood of complications, such as fibrosis and malignancy, is essential for improving clinical outcomes in UC patients. Bioinformatics approaches have proven valuable in uncovering the immune cell signatures that underlie the pathogenesis of UC, offering promising diagnostic tools and potential therapeutic targets to modulate the immune response and prevent long-term damage.

Ulcerative colitis frequently advances without noticeable symptoms, leading to considerable tissue damage before a diagnosis is made. This highlights the urgent need for the identification of molecular markers specific to ulcerative colitis, which would facilitate early diagnosis and enable timely therapeutic interventions. Building on this premise, this study aimed to identify molecular markers associated with ulcerative colitis (UC) and utilized both a dextran sulfate sodium (DSS)-induced UC rat model and clinical samples from UC patients for experimental validation.

The results demonstrated that NCF2 expression was significantly elevated in the colon tissue of rats with ulcerative colitis (UC) and in clinical samples from UC patients. NCF2 plays a key role in immune and inflammatory responses by regulating NADPH oxidase-mediated ROS production, influencing inflammasome activation, MAPK signaling, and anti-tumor immunity.[42,43] The increase in NCF2 expression may reflect an adaptive mechanism of macrophages responding to the inflammatory environment characteristic of UC. Furthermore, the association between NCF2 and macrophage activation highlights the potential of targeting this pathway for therapeutic intervention. Previous studies have indicated that macrophages in UC exhibit a pro-inflammatory phenotype, contributing to epithelial barrier dysfunction and the perpetuation of the inflammatory cycle.[44] The upregulation of NCF2 may further enhance this inflammatory response through increased ROS production, leading to oxidative stress and subsequent tissue damage. These findings warrant further investigation into the specific mechanisms by which NCF2 influences macrophage behavior and its potential as a biomarker for disease severity or therapeutic targets in UC. Its involvement may contribute to inflammation and tissue remodeling seen in UC, highlighting its potential significance in the disease's progression and as a target for therapeutic strategies.

Our findings position NCF2 as a promising translational target for ulcerative colitis (UC), with dual potential for both diagnostic and therapeutic development. The consistent upregulation of NCF2 in preclinical and clinical settings supports its utility as a non-invasive biomarker, where blood-based detection of NCF2 expression in peripheral blood mononuclear cells or serum exosomes could enable disease monitoring and patient stratification. Therapeutically, targeting NCF2 offers a novel approach to modulate oxidative stress and macrophage-driven inflammation, through strategies such as small-molecule inhibitors disrupting NADPH oxidase assembly or RNA-based therapies for tissue-specific silencing. Future efforts should focus on validating NCF2-based detection assays in longitudinal cohorts and evaluating targeted interventions in disease-relevant models to advance these translational applications.

Conclusion

This study systematically identifies and validates NCF2 as a novel diagnostic biomarker for ulcerative colitis (UC), demonstrating its significant association with immune dysregulation and macrophage infiltration through comprehensive bioinformatic analysis and experimental validation in both murine models and human tissues. These findings provide

crucial insights into UC pathogenesis and offer a potential target for early diagnosis. To advance the clinical translation of these results, we propose developing a standardized blood-based assay (eg, ELISA or RT-qPCR) to quantify NCF2 levels in peripheral blood, enabling a minimally invasive diagnostic approach. Further validation through large-scale, prospective, multi-center studies will be essential to establish diagnostic thresholds, correlate NCF2 expression with disease activity, and evaluate its utility across diverse populations. Despite limitations such as incomplete clinical metadata and the need for deeper exploration of miRNA interactions, this work establishes a foundational framework for leveraging NCF2 as a clinically actionable biomarker in UC management.

Data Sharing Statement

The datasets generated and/or analyzed during the current study are available in the GEO repository, https://www.ncbi.nlm.nih.gov/geo/query/acc.cgi?acc=GSE38713, https://www.ncbi.nlm.nih.gov/geo/query/acc.cgi?acc=GSE92415, https://www.ncbi.nlm.nih.gov/geo/query/acc.cgi?acc=GSE87466, https://www.ncbi.nlm.nih.gov/geo/query/acc.cgi?acc=GSE119600.

Ethics Statement

The current study was conducted in accordance with the principles outlined in the Declaration of Helsinki. Approval for the animal research was granted by the Ethics Committee of the Experimental Animal Center at Yangzhou University School of Medicine (approval no. YXYLL-2024-077). All animal experiments were conducted in accordance with the National Institutes of Health Guide for the Care and Use of Laboratory Animals (Eighth Edition). Additionally, the human-related experiments received approval from the Ethics Committee of the Affiliated Hospital of Yangzhou University (approval no. 2022-YKL7). Written informed consent was obtained from all patients for the inclusion of their samples in the biobank.

Acknowledgments

The authors thank the GEO database for making their datasets publicly available. We appreciate the technical support and institutional resources provided by Yangzhou University Affiliated Hospital and Yangzhou University School of Medicine. We extend our sincere gratitude to Professor Yanbing Ding of the Affiliated Hospital of Yangzhou University, who served as the principal applicant for the animal study ethics approval and provided oversight and methodological guidance throughout this project. We also thank Professor Guotao Lu, from the same institution, who acted as the principal applicant for the ethics approval of the human research component and offered valuable advice during the study.

Disclosure

The authors report no conflicts of interest in this work.

References

1. Ye Y, Pang Z, Chen W, et al. The epidemiology and risk factors of inflammatory bowel disease. *Int J Clin Exp Med*. 2015;8(12):22529–22542.
2. Kaplan GG. The global burden of IBD: from 2015 to 2025. *Nat Rev Gastroenterol Hepatol*. 2015;12(12):720–727. doi:10.1038/nrgastro.2015.150
3. Yu J, Cheon JH. Microbial Modulation in Inflammatory Bowel Diseases. *Immune Netw*. 2022;22(6):e44. doi:10.4110/in.2022.22.e44
4. El-Sayed A, Kapila D, Taha RSI, et al. The Role of the Gut Microbiome in Inflammatory Bowel Disease: the Middle East Perspective. *J Pers Med*. 2024;14(6):652. doi:10.3390/jpm14060652
5. Rogler G, Singh A, Kavanaugh A, et al. Extraintestinal Manifestations of Inflammatory Bowel Disease: current Concepts, Treatment, and Implications for Disease Management. *Gastroenterology*. 2021;161(4):1118–1132. doi:10.1053/j.gastro.2021.07.042
6. Yu P, Shen F, Zhang X, et al. Association of single nucleotide polymorphisms of IL23R and IL17 with ulcerative colitis risk in a Chinese Han population. *PLoS One*. 2012;7(9):e44380. doi:10.1371/journal.pone.0044380
7. Kryczek I, Wang L, Wu K, et al. Inflammatory regulatory T cells in the microenvironments of ulcerative colitis and colon carcinoma. *Oncoimmunology*. 2016;5(8):e1105430. doi:10.1080/2162402X.2015.1105430
8. Tsuchiya M, Kobayashi K, Aiso S, et al. Clinical features and management of 7 cases of toxic megacolon. *Nihon Shokakibyo Gakkai Zasshi*. 1983;80(9):1735–1746.
9. Berre CL, Honap S, Peyrin-Biroulet L. Ulcerative colitis. *Lancet*. 2023;402(10401):571–584. doi:10.1016/S0140-6736(23)00966-2
10. Liu H, Dasgupta S, Fu Y, et al. Subsets of mononuclear phagocytes are enriched in the inflamed colons of patients with IBD. *BMC Immunol*. 2019;20(1):42. doi:10.1186/s12865-019-0322-z
11. Soubières AA, Poullis A. A A Soubières, A Poullis. Emerging Biomarkers for the Diagnosis and Monitoring of Inflammatory Bowel Diseases. *Inflamm Bowel Dis*. 2016;22(8):2016–2022. doi:10.1097/MIB.0000000000000836

12. Lazarov T, Juarez-Carreño S, Cox N, et al. Physiology and diseases of tissue-resident macrophages. *Nature*. 2023;618(7966):698–707. doi:10.1038/s41586-023-06002-x
13. Wen JH, Li DY, Liang S, et al. Macrophage autophagy in macrophage polarization, chronic inflammation and organ fibrosis. *Front Immunol*. 2022;13:946832. doi:10.3389/fimmu.2022.946832
14. Saez A, Herrero-Fernandez B, Gomez-Bris R, et al. Pathophysiology of Inflammatory Bowel Disease: innate Immune System. *Int J Mol Sci*. 2023;24(2):1526. doi:10.3390/ijms24021526
15. Zhang M, Li X, Zhang Q, et al. Roles of macrophages on ulcerative colitis and colitis-associated colorectal cancer. *Front Immunol*. 2023;14:1103617. doi:10.3389/fimmu.2023.1103617
16. Kim MK, Kim J. Properties of immature and mature dendritic cells: phenotype, morphology, phagocytosis, and migration. *RSC Adv*. 2019;9(20):11230–11238. doi:10.1039/C9RA00818G
17. Pergolizzi S, Rizzo G, Favaloro A, et al. Expression of VAChT and 5-HT in Ulcerative colitis dendritic cells. *Acta Histochem*. 2021;123(4):151715. doi:10.1016/j.acthis.2021.151715
18. Apolit C, Campos N, Vautrin A, et al. ABX464 (Obefazimod) Upregulates miR-124 to Reduce Proinflammatory Markers in Inflammatory Bowel Diseases. *Clin Transl Gastroenterol*. 2023;14(4):e00560. doi:10.14309/ctg.0000000000000560
19. Nguyen J, Finkelman BS, Escobar D, et al. Overexpression of programmed death ligand 1 in refractory inflammatory bowel disease. *Hum Pathol*. 2022;126:19–27. doi:10.1016/j.humpath.2022.04.011
20. Zhou J, Liu J, Gao Y, et al. miRNA-Based Potential Biomarkers and New Molecular Insights in Ulcerative Colitis. *Front Pharmacol*. 2021;12:707776. doi:10.3389/fphar.2021.707776
21. Roth IL, Salamon P, Freund T, et al. Novel NCF2 Mutation Causing Chronic Granulomatous Disease. *J Clin Immunol*. 2020;40(7):977–986. doi:10.1007/s10875-020-00820-8
22. Bakutenko IY, Haurylchyk ID, Nikitchenko NV, et al. Neutrophil cytosolic factor 2 (NCF2) gene polymorphism is associated with juvenile-onset systemic lupus erythematosus, but probably not with other autoimmune rheumatic diseases in children. *Mol Genet Genomic Med*. 2022;10(1):e1859. doi:10.1002/mgg3.1859
23. Shi K, Zhou J, Li M, et al. Pan-cancer analysis of PLAU indicates its potential prognostic value and correlation with neutrophil infiltration in BLCA. *Biochim Biophys Acta Mol Basis Dis*. 2024;1870(2):166965. doi:10.1016/j.bbadis.2023.166965
24. Chen G, Sun J, Xie M, et al. PLAU Promotes Cell Proliferation and Epithelial-Mesenchymal Transition in Head and Neck Squamous Cell Carcinoma. *Front Genet*. 2021;12:651882. doi:10.3389/fgene.2021.651882
25. Kałużna A, Olczyk P, Komosińska-Vassev K. The Role of Innate and Adaptive Immune Cells in the Pathogenesis and Development of the Inflammatory Response in Ulcerative Colitis. *J Clin Med*. 2022;11(2):400. doi:10.3390/jcm11020400
26. Lopes TCM, Mosser DM, Gonçalves R. Macrophage polarization in intestinal inflammation and gut homeostasis. *Inflamm Res*. 2020;69(12):1163–1172. doi:10.1007/s00011-020-01398-y
27. Andoh A, Tsujikawa T, Inatomi O, et al. Leukocytapheresis therapy modulates circulating t cell subsets in patients with ulcerative colitis. *Ther Apher Dial*. 2005;9(3):270–276. doi:10.1111/j.1774-9987.2005.00270.x
28. Dotan I, Rachmilewitz D. Probiotics in inflammatory bowel disease: possible mechanisms of action. *Curr Opin Gastroenterol*. 2005;21(4):426–430.
29. Chang X, Song YH, Xia T, et al. Macrophage-derived exosomes promote intestinal mucosal barrier dysfunction in inflammatory bowel disease by regulating TMIGD1 via mircroRNA-223. *Int Immunopharmacol*. 2023;121:110447. doi:10.1016/j.intimp.2023.110447
30. Chen X, Zhang M, Zhou F, et al. SIRT3 Activator Honokiol Inhibits Th17 Cell Differentiation and Alleviates Colitis. *Inflamm Bowel Dis*. 2023;29(12):1929–1940. doi:10.1093/ibd/izad099
31. Feng B, Xu L, Song S, et al. ER stress modulates the immune regulatory ability in gut M2 cells of patients with ulcerative colitis. *iScience*. 2023;26(4):106498. doi:10.1016/j.isci.2023.106498
32. Sun L, Wang X, Saredy J, et al. Innate-adaptive immunity interplay and redox regulation in immune response. *Redox Biol*. 2020;37:101759. doi:10.1016/j.redox.2020.101759
33. Muise AM, Xu W, Guo CH, et al. NADPH oxidase complex and IBD candidate gene studies: identification of a rare variant in NCF2 that results in reduced binding to RAC2. *Gut*. 2012;61(7):1028–1035. doi:10.1136/gutjnl-2011-300078
34. Yan X, Meng L, Zhang X, et al. Reactive oxygen species-responsive nanocarrier ameliorates murine colitis by intervening colonic innate and adaptive immune responses. *Mol Ther*. 2023;31(5):1383–1401. doi:10.1016/j.ymthe.2023.02.017
35. Gluschko A, Farid A, Herb M, et al. Macrophages target Listeria monocytogenes by two discrete non-canonical autophagy pathways. *Autophagy*. 2022;18(5):1090–1107. doi:10.1080/15548627.2021.1969765
36. Ascic E, Åkerström F, Nair MS, et al. In vivo dendritic cell reprogramming for cancer immunotherapy. *Science*. 2024;386(6719):eadn9083. doi:10.1126/science.adn9083
37. Saez A, Gomez-Bris R, Herrero-Fernandez B, et al. Innate Lymphoid Cells in Intestinal Homeostasis and Inflammatory Bowel Disease. *Int J Mol Sci*. 2021;22(14):7618. doi:10.3390/ijms22147618
38. Derkacz A, Olczyk P, Olczyk K, et al. The Role of Extracellular Matrix Components in Inflammatory Bowel Diseases. *J Clin Med*. 2021;10(5):1122. doi:10.3390/jcm10051122
39. Aust DE, Baretton GB, Sommer U. Ulcerative colitis-associated carcinogenesis: an update. *Pathologie*. 2023;44(5):294–300. doi:10.1007/s00292-023-01207-3
40. Rieder F, Mukherjee PK, Massey WJ, et al. Fibrosis in IBD: from pathogenesis to therapeutic targets. *Gut*. 2024;73(5):854–866. doi:10.1136/gutjnl-2023-329963
41. Méndez JEP, Pérez SIJ, Marcacuzco HTV, et al. Medical and surgical management of moderate-to-severe inflamatory bowel disease. *Rev Gastroenterol Peru*. 2021;41(2):79–85.
42. Nunoi H, Nakamura H, Nishimura T, et al. Recent topics and advanced therapies in chronic granulomatous disease. *Hum Cell*. 2023;36(2):515–527. doi:10.1007/s13577-022-00846-7
43. Li L, Mao R, Yuan S, et al. NCF4 attenuates colorectal cancer progression by modulating inflammasome activation and immune surveillance. *Nat Commun*. 2024;15(1):5170. doi:10.1038/s41467-024-49549-7
44. Dharmasiri S, Garrido-Martin EM, Harris RJ, et al. Human Intestinal Macrophages Are Involved in the Pathology of Both Ulcerative Colitis and Crohn Disease. *Inflamm Bowel Dis*. 2021;27(10):1641–1652. doi:10.1093/ibd/izab029